Ab initio density-functional study of NO adsorption on close-packed transition and noble metal surfaces: II. Dissociative adsorption

2006 J. Phys.: Condens. Matter 18 41

(http://iopscience.iop.org/0953-8984/18/1/003)

INSTITUTE OF PHYSICS PUBLISHING JOURNAL OF PHYSICS: CONDENSED MATTER

J. Phys.: Condens. Matter **18** (2006) 41–54 doi:10.1088/0953-8984/18/1/003

Ab initio density-functional study of NO adsorption on close-packed transition and noble metal surfaces: II. Dissociative adsorption

Marek Gajdoš, Jürgen Hafner and Andreas Eichler

Institut für Materialphysik and Center for Computational Materials Science, Universität Wien, Sensengasse 8/12, A-1090 Wien, Austria

E-mail: Marek.Gajdos@univie.ac.at and Juergen.Hafner@univie.ac.at

Received 4 August 2005
Published 9 December 2005
Online at stacks.iop.org/JPhysCM/18/41

Abstract

Following our investigation of molecular NO adsorption (Gajdos *et al* 2006 *J. Phys.: Condens. Matter* **18** 13), the dissociation of NO molecules on the close-packed surfaces of late transition (Co, Ni, Ru, Rh, Pd, Ir, Pt) and noble (Cu, Ag, Au) metals has been studied using first-principles density functional calculations. The nudged-elastic-band method has been used for the determination of the transition states. Our results demonstrate that the transition-state energies show a linear dependence on the dissociative chemisorption energies according to the Brønsted–Evans–Polanyi rule. The validity of this linear relationship is shown to arise from the geometrical similarity of the transition states on all metals, which are very close to the final state geometries.

(Some figures in this article are in colour only in the electronic version)

1. Introduction

The interaction of diatomic molecules (CO, N_2, NO, H_2, O_2, ...) with transition and noble metals is a particularly interesting area of surface science and catalysis. The adsorbate–surface interaction can lead to the breaking and making of chemical bonds and trigger important surface catalysed reactions. In particular, the decomposition of NO in conventional automotive catalytic converters is an important technological problem. A good exhaust catalyst should favour dissociation of NO leading to the recombination of atomic nitrogen to N_2, followed by desorption. At the same time adsorption of CO should be non-dissociative and facilitate oxidation of adsorbed CO to CO_2. According to the results compiled by Broden *et al* [1] (see also Brown and King [2]), for CO the dividing line between dissociative and molecular adsorption passes between Fe/Co, Tc/Ru and W/Re, while for NO it is shifted to the right: a clear preference for molecular adsorption has been found only on Pd and Pt, while for

Ni and Ir coexistence of molecular and dissociative adsorption has been reported. It is now generally accepted [3, 4] that the NO reduction process on late transition metals consists of the following steps: (1) NO dissociation (NO $\longrightarrow$ N + O); (2) N_2 formation (N + N $\longrightarrow$ N_2); (3) O removal, e.g. reduction by CO (CO + O $\longrightarrow$ CO_2) or NO (NO + O $\longrightarrow$ NO_2); (4) formation of other by-products such as N_2O. The rate-controlling step is the dissociation of NO. Practical catalysts contain Pt and Rh; their activity can be explained by low barriers for NO dissociation, while the barriers for CO dissociation are high enough to favour molecular adsorption.

In two recent papers (Gajdos *et al* [5] and the preceding paper in this volume [6]) we have used *ab initio* density-functional calculations to study the molecular adsorption of CO and NO on the close-packed surfaces ((111) on face-centred cubic, (0001) on hexagonal-close-packed structures) of late transition metals (Co, Ni, Ru, Rh, Pd, Ir, Pt) and noble metals (Cu, Ag, Au). A comprehensive investigation of the adsorption of these two important molecules on a series of substrates allows us to identify the important trends in the adsorption energies, geometries, and vibrational properties of the adsorbate–substrate complex and leads to a better understanding of the differences in the adsorption behaviour of CO and NO. In the present work we extend these investigations to the dissociation of NO.

To date *ab initio* density-functional techniques have been applied to study NO dissociation on a number of clean metal surfaces: Pd and Rh surfaces by Loffreda *et al* [7]; Rh, Pd, and Ru surfaces by Hammer *et al* [8–11]; on Pt by Eichler and Hafner [12, 13]; on Ir and Pt surfaces by Liu *et al* [14, 15]. In the work of Eichler and Hafner, the investigations have been extended to cover the NO + CO redox reaction [12, 13]; Liu *et al* [14, 15] have considered the selective oxidation of NO under excess oxygen. The comparison of NO dissociation with dissociation reactions of CO and N_2 suggests that these dissociation reactions possess some common features: (1) the transition state for these dissociation reactions belongs to the *late* transition states, i.e. the reaction barrier is largely determined by the adsorption energy of the products. This was found not only in the studies of NO dissociation cited above, but also for CO dissociation on close-packed Ru, Rh, Pd, Os, Ir, and Pt surfaces [16] and by Logadottir *et al* [17, 18] for N_2 dissociation on Pd, Cu, Fe, Ru, and Mo surfaces. (2) Dissociation reactions, and NO dissociation in particular, are highly structure sensitive. Open surfaces or vicinal surfaces with steps and edges are generally much more reactive than close-packed flat surfaces. A strong reduction of the dissociation barrier for NO at steps on the surfaces of Pd [7, 8, 10], Ru [9, 19], and Pt [20, 21] has been reported. Liu and Hu [14] have extended these considerations and formulated general rules for the structure-sensitivity of catalytic reactions on metal surfaces. In particular, they pointed out that dissociation reactions are always much more structure sensitive than the reverse association reactions. (3) Diatomic dissociation reactions are coverage dependent—very often dissociative adsorption at low coverage changes to molecular adsorption at higher coverage. This may be explained by the space required to accommodate the dissociation products.

The DFT calculations of the potential energy profiles of dissociation reactions suggest the existence of an essentially linear relationship between the transition-state energy E_{TS} for dissociation and the binding energy $E_{ads,prod}$ of the dissociated reaction products (or dissociative chemisorption energy) on the surface of the catalyst, which is independent of the reactant and of the metal but varies with the structure of the active site [16, 18, 22, 23]. Such a behaviour is usually known as the Brønsted–Evans–Polanyi (BEP) relation [24, 25] or linear-free-energy relation,

$$E_{TS} = A + B \cdot E_{ads,prod}. \tag{1}$$

BEP relations have been empirically established for a number of chemical reactions. The connection between the activation energy and the reaction enthalpy is often discussed in terms

of the Hammond principle [26] which states that for highly exothermic reactions the transition state (TS) is structurally similar to the reactant (early TS), while in highly endothermic reactions the product is more similar to the transition state (late TS). From this point of view the existence of a BEP relation between the reaction barrier and the reaction enthalpy for the dissociation of diatomic molecules is rather surprising, since in many cases the dissociated atoms are more strongly bound to the surface than the adsorbed molecule. From the Hammond principle one would therefore expect the dissociation proceeding via a chemisorbed molecular species to have an early transition state whose structure should be closer to that of the molecular precursor than to the dissociated molecule in the final state.

The present paper is devoted to a detailed investigation of the potential-energy profile for the dissociation of NO on the close-packed surfaces of seven late transition metals and of the noble metals. The previous DFT studies that lead to the formulation of the BEP relation for diatomic dissociation reactions furnish data for a large number of different systems, but only the work of Liu and Hu [16] on CO dissociation on transition metals allows us to follow the trend as a function of the properties of the metallic substrate. Interestingly, a different BEP relation (different slope of the linear correlation between E_{TS} and $E_{\mathrm{ads,prod}}$) has been found for 4d and 5d metals. Such a difference would contradict the postulated 'universality' of BEP relations for diatomic reactions [17, 23]. Here we report results on all the late 3d, 4d, and 5d transition and noble metals on which a molecular adsorption precedes NO dissociation. Detailed results on molecular adsorption have already been presented [6]—hereafter this paper will be referred to as I. Here we concentrate on the determination of the transition states for dissociation and we discuss the results in the light of a possible Brønsted–Evans–Polanyi relation.

Our paper is organized as follows. In section 2 we briefly review the computational aspects (as far as not covered in I) and we introduce the strategy for transition-state determination. In section 3 we discuss the general scenario for NO dissociation; section 4 presents our results for the potential-energy profiles and the transition-state energies and geometries on the various metal surfaces, compared to the available experimental observations. Section 5 discusses the trends, and in particular the correlation between the transition-state energies and final-state adsorption energies as postulated by the BEP relation. The last section summarizes our conclusions.

2. Methodology

The calculations in this work are performed using the Vienna *Ab Initio* Simulation Package VASP [27, 28], which is based on density functional theory (DFT) and uses a plane-wave basis set. The electron–ion interaction is described using the projector-augmented-wave (PAW) method [29, 30] with plane waves up to an energy of $E_{\mathrm{cut}} = 450$ eV. For the exchange and correlation functional the form proposed by Perdew and Zunger [31] is used, adding (semi-local) generalized gradient corrections (GGA) according to Perdew *et al* (PW91) [32].

The dissociation of NO is characterized by a free space requirement: free adsorption sites for the dissociation products must be available in the vicinity of the adsorbed molecule. Therefore, the dissociation of NO was studied using a c(4×4) surface cell, leading to a coverage of 0.125 ML, while our studies of molecular adsorption had been performed using a p(2×2) surface cell and a coverage of 0.25 ML. The lower molecular coverage facilitates dissociation and yields activation energies which are independent of lateral interactions.

Brillouin-zone integration have been performed with a ($2 \times 3 \times 1$) Γ-centred k-point mesh. Other details of our computational set-up details remain as specified in our paper on CO adsorption [5]. The slab representing the surface consists of four monolayers of metal and NO is adsorbed on one side only. The two uppermost metal layers are allowed to relax—as a rule,

substrate relaxation is more important for the adsorption of the dissociated atoms which bind very strongly to the substrate than for the molecular precursor. A conjugate-gradient algorithm is used to relax ions to their ground state locations [33]. Equilibrium is reached if the force on the atoms becomes less than 0.1 eV Å^{-1} in each of the Cartesian directions. Vibrational properties were computed for the initial and the transition states by applying a finite difference method where the substrate is frozen and NO is allowed to vibrate in any direction. If the molecule is in a true transition state it must have one, and only one, imaginary frequency corresponding to the N–O stretching mode.

Dissociation paths and diffusion barriers are determined using the nudged elastic band (NEB) method [34, 35]. In the NEB method a reaction coordinate relating initial (molecular) and final (dissociated) states is defined and a set of intermediate states is distributed along the reaction path. Each intermediate state is fully relaxed in the hyperspace perpendicular to the reaction coordinate. In the interval between the states with the highest potential energies, the search has been refined using the climbing-image NEB method [36, 37]. For the transition state, the vibrational spectrum has been calculated—if the criterion of a single imaginary eigenmode is not satisfied, the search is further refined. The climbing-image NEB method, combined with the vibrational analysis, leads to a very precise determination of the transition state.

In the product state, N and O atoms are adsorbed in threefold hollows separated by a rather short distance. To determine the contribution E_{int} of the intramolecular N–O interactions to the final-state and transition-state energies, separate calculations of N and O adsorption have been performed in a smaller p(2 × 2) surface cell. The interaction energy is determined by $E_{\mathrm{ads,N+O}} = (E_{\mathrm{ads,N}} + E_{\mathrm{ads,O}} + \Delta) + E_{\mathrm{int}}$, where $E_{\mathrm{ads,N}}$ and $E_{\mathrm{ads,O}}$ are the atomic adsorption energies calculated relative to the gas-phase molecules N_2 and O_2, and $\Delta = E_{\mathrm{NO}}(\mathrm{g}) - \frac{1}{2}[E_{\mathrm{O_2}}(\mathrm{g}) + E_{\mathrm{N_2}}(\mathrm{g})]$ corrects for the difference in the gas-phase binding energies of the molecules. The gas-phase binding energies have been calculated for molecules in a large box of 12 × 13 × 14 Å^3, with appropriate aspherical and dipolar corrections. The calculated atomization energies of the O_2, N_2, and NO molecules are 6.427/12.789/7.660 eV, to be compared with experimental values of 5.12/9.85/6.64 eV—it is well known that the DFT error in molecular binding energies is always much larger than for solid-state calculations.

3. Reaction pathway for NO dissociation

Two models have been proposed to describe the dissociation of a molecule on a surface—direct dissociation and dissociation via a molecular precursor. In direct dissociative chemisorption the incident molecule decomposes into the constituent molecules immediately upon impact on the surface. In a precursor-mediated adsorption the molecule is adsorbed interact before dissociation. The formation of a molecular precursor state results from the loss of kinetic energy of the incident molecule upon collision with the surface. The molecule remains in this chemisorbed state until it receives enough energy from the catalyst to reorient into a configuration favouring dissociation or desorption without dissociation. The favoured mechanism for dissociation is determined by the potential energy surface (PES) of the molecule interacting with the surface.

A schematic PES is shown in figure 1. The reference-energy is given by the molecule in the gas phase. Molecular adsorption of NO on metallic surfaces is usually an exothermic process, characterized by the molecular adsorption energy $E_{\mathrm{ads,NO}}$. Dissociation of the chemisorbed molecule is an activated process passing through a transition state with energy E_{TS}; the *true activation energy* relative to the chemisorbed initial state is $E_{\mathrm{diss}} = E_{\mathrm{TS}} - E_{\mathrm{ads,NO}}$, whereas the energy of the transition state measures the *apparent activation energy* relative to the molecule

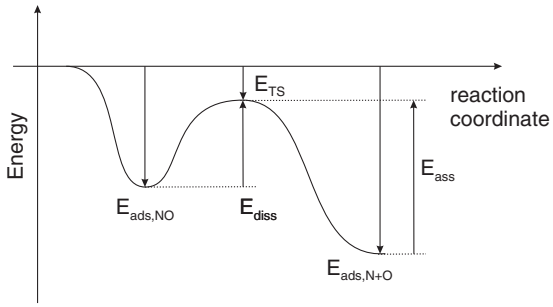

Figure 1. Potential energy profile for the dissociation of NO (schematic); cf text.

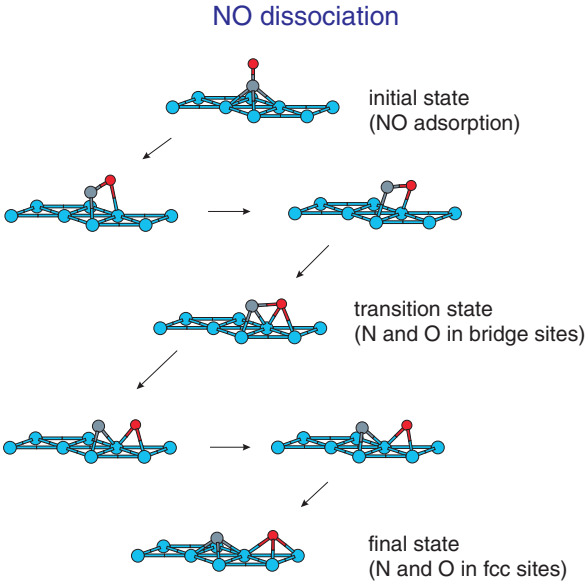

Figure 2. Reaction pathway for the dissociation of NO on a close-packed (111) surface. The example shown in the figure refers to NO dissociation on Pt, starting from a molecule adsorbed in a fcc hollow; cf text.

in the gas phase. The final-state energy is given by the energy of the co-adsorbed atoms, $E_{\mathrm{ads,N+O}}$; it differs from the sum of the adsorption energies of the isolated atoms, $E_{\mathrm{ads,N}}+E_{\mathrm{ads,O}}$, by an interaction energy E_{int} depending on the interatomic distance between N and O. The reverse process, the associative formation of a NO molecule from the co-adsorbed atoms, has an activation energy $E_{\mathrm{ass}} = E_{\mathrm{TS}} - E_{\mathrm{ads,N+O}}$. Direct dissociation is favoured only if the transition-state energy is negative and lower or comparable to the molecular chemisorption energy $E_{\mathrm{ads,NO}}$. This is not the case for any of the metallic surfaces considered here.

The crucial point is the determination of the transition state. Our calculations using the NEB method lead to the following reaction scenario (see figure 2). (1) in the initial state the molecule is adsorbed in a threefold hollow (fcc or hcp) with the molecular axis perpendicular to the surface. (2) The reaction starts by moving the N atom slightly out of the centre of the hollow and tilting the molecular axis such that the oxygen atom binds to a neighbouring atom. (3) In the transition state the molecule is almost parallel to the surface; both the N and the

O atom are close to bridge positions, shifted towards their final positions in the hollows. In such a TS on a flat surface both atoms share a common surface atom—this is important for understanding the structure sensitivity of the reaction. (4) After the molecular bond has been broken, both atoms move to the closest hollow sites. In the final state both the N and the O atom are bound in a hollow of the same type as occupied by the initial state. The adsorbed atoms still share a bonding surface atom. (5) The dissociation can take place only if at least two free hollow positions are available close to the site occupied by the adsorbed molecule. But even then, the activation and reaction energies will be influenced by lateral interactions. This explains the strong coverage dependence of NO dissociation. The scenario for NO dissociation sketched here is in general agreement with the results of previous studies [19, 38].

It is important to note that in the molecularly chemisorbed state the activation of the molecule for dissociation is only modest—as shown by a small elongation of the N–O bond from 1.168 Å in the gas phase to 1.19 → 1.23 Å, and by a modest red-shift of the N–O stretching mode by only 300 → 400 cm^{-1} (see I for details). Hence a late TS closely resembling the final state has to be expected.

4. Transition states for NO dissociation

The optimized potential-energy profiles for NO dissociation on the surfaces of the 3d, 4d, and 5d metals are shown in figure 3. Initial-, transition-, and final-state energies, as well as the activation energies for dissociation and association, are summarized in table 1.

The initial state is the NO molecule in the chemisorbed state on the surface. The most favoured adsorption site of the NO molecule on the close-packed transition- and noble-metal surfaces is a threefold hollow site. For the transition metals the molecular chemisorption energy for this low coverage of $\frac{1}{8}$ ML varies between −2.65 eV on Ru(0001) and −2.07 eV on Pt(111); for the noble metals a much weaker chemisorption varying between −1.22 eV on Cu(111) and −0.38 eV on Au(111) is calculated. As a rule, the chemisorption energies reported here are slightly more exothermic (by about 0.1–0.2 eV) than the values for $\frac{1}{4}$ ML coverage presented in I. The preferred absorption site is the hcp site for the elements which are more to the left in the periodic table (Co, Ru, Rh) and the fcc site for the other metals, with the exception of Ir and Au, where the top site is slightly favoured (for any details see I). To make it easier to follow the general trends, NO in an fcc hollow was also used as the initial state for these two metals.

4.1. Transition-state and reaction energies

The potential-energy profiles calculated for the transition-metal surfaces show a characteristic variation across the transition-metal series: with increasing band filling dissociation becomes less exothermic (it is even weakly endothermic for Pd and Pt), the transition state is shifted increasingly towards the final state, and the true activation energy for dissociation increases quite dramatically, from $E_{diss} = 0.73$ eV on Co(0001) to $E_{diss} = 2.77$ eV on Pd(111). In contrast, the activation energy for the reverse reaction, the association of nitrogen and oxygen atoms to form NO, varies only between $E_{ass} = 1.83$ eV [Co(0001)] and $E_{ass} = 2.19$ eV [Pt(111)].

On the heavy noble metals, molecular chemisorption is rather weak; the transition-state energies and final-state energies are large and positive so that desorption will always occur before dissociation can take place. On Cu NO dissociation is weakly endothermic; the transition-state energy is only slightly more positive than on Pt or Pd. Hence NO dissociation on Cu shows more similarity with the heavy metals of the Pt group than with the heavy noble metals.

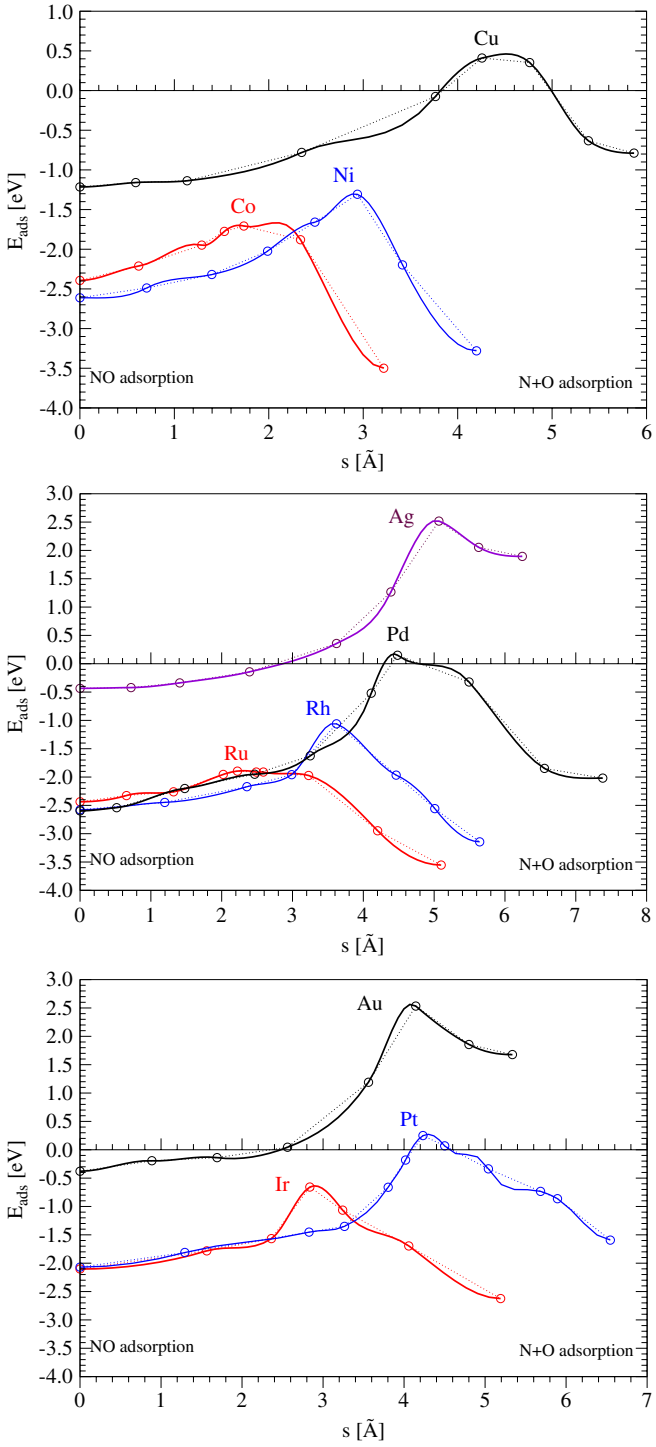

Figure 3. Potential energy profile for the dissociation reaction of NO on the surfaces of the 3d (top), 4d (centre) and 5d (bottom) transition and noble metals. The open circles mark the intermediates along the reaction channel whose structures and energies have been optimized in the hyperspace perpendicular to the reaction coordinate; the full lines show a spline-fit of the energy profile.

Table 1. Energies along the reaction path for NO dissociation (all in eV per N–O dimer): adsorption energy of chemisorbed NO, $E_{ads,NO}$, transition-state energy E_{TS} and final-state energy $E_{ads,N+O}$ of the co-adsorbed N and O atoms. In addition, the table summarizes the heat of reaction E_{react}, the activation energies E_{diss} and E_{ass} for NO dissociation and N+O association. The reference energy is the gas-phase NO molecule. All energies are given in eV. All the values are according to transition paths for the dissociation depicted in figures 3.

Surface	$E_{ads,NO}$	E_{TS}	$E_{ads,N+O}$	E_{react}	E_{diss}	E_{ass}	Ref.	Functional
Co	−2.39	−1.67	−3.50	−1.11	0.73	1.83		PW91
Ni	−2.61	−1.30	−3.28	−0.67	1.31	1.98		PW91
Cu	−1.22	0.46	−0.79	0.43	1.68	1.25		PW91
	−1.35	−0.15			1.20		[38]	PW91
Ru	−2.65	−1.90	−3.60	−0.95	0.75	1.70		PW91
	−2.73	−1.45			1.28		[9, 19]	PW91
	−2.24	−0.83			1.44		[9, 19]	RPBE
Rh	−2.58	−1.06	−3.14	−0.56	1.52	2.08		PW91
	−2.50	−0.89			1.61		[7]	PW91
	−2.45	−0.85			1.60		[11]	PW91
Pd	−2.59	0.17	−2.02	0.57	2.77	2.19		PW91
	−2.30	0.17			2.47		[7]	PW91
	−2.29	0.31			2.60		[10]	PW91
	−1.80	0.90			2.70		[10]	RPBE
Ag	−0.43	2.52	1.89	2.32	2.95	0.63		PW91
Ir	−2.10	−0.64	−2.62	−0.52	1.46	1.98		PW91
	−2.10	−0.64			1.46		[14]	PW91
Pt	−2.07	0.27	−1.59	0.48	2.34	1.86		PW91
	−1.98	0.49	−1.65	0.33	2.47	1.99	[21]	PW91
	−2.02	0.08			2.10		[38]	PW91
	−2.05	0.55			2.60		[14]	PW91
Au	−0.38	2.70	1.68	2.06	3.08	1.02		PW91

The trends in the reaction energies are largely determined by the adsorption energies $E_{ads,N}$ and $E_{ads,O}$ of the isolated N and O atoms. The atomic adsorption energies at the high-symmetry sites of the close-packed surfaces, calculated relative to the gas-phase molecules N_2 and O_2, are summarized in table 2. For adsorption in the threefold hollows, the two top layers of the substrate have been relaxed. We find that while dissociative adsorption of oxygen is always exothermic (with the sole exception of Au), dissociative adsorption of nitrogen is weakly exothermic only on Co, Ni, Ru, Rh, and Ir, weakly endothermic on Pd and Pt, and strongly endothermic on the noble metals. Site preference is hcp for both atomic species on Co and Rh and fcc for both metals on Ni, Pd, Pt, and the noble metals. On Rh and Ir nitrogen adsorbs preferentially in the hcp, and oxygen in an fcc hollow. Following Hammer [9] we define a rebonding potential energy E_{rebond} for the reaction products according to

$$E_{rebond} = E_{ads,N} + E_{ads,O} + \Delta \tag{2}$$

where $\Delta = E_{NO}(g) - \frac{1}{2}[E_{O_2}(g) + E_{N_2}(g)] = -0.95$ eV shifts the energy zero to the gas-phase NO molecule. The energies of the product and transition states may be decomposed according to

$$E_{TS} = E_{rebond} + E_{int,TS} \tag{3}$$

and

$$E_{prod} = E_{rebond} + E_{int,prod} \tag{4}$$

Table 2. Adsorption energies of isolated N and O atoms in high-symmetry sites on the close-packed surfaces of noble and transition metals (calculated relative to the gas-phase molecules N_2 and O_2), E_{rebond} measuring the sum of the atomic adsorption energies relative to the gas-phase NO molecule; $E_{\text{int,prod}}$ and $E_{\text{int,TS}}$ represent the strength of the intramolecular interaction in the product and transition states; cf text. All energies are given in eV.

Metal	Atom (site)	$E_{\text{ads,atom}}$	E_{rebond}	$E_{\text{int,prod}}$	$E_{\text{int,TS}}$
Co	N(hcp)	−0.44	−3.99	0.49	2.32
	O(hcp)	−2.60			
Ni	N(fcc)	−0.14	−3.44	0.16	2.14
	O(fcc)	−2.35			
Cu	N(fcc)	1.37	−1.13	0.44	1.59
	O(fcc)	−1.55			
Ru	N(hcp)	−0.94	−4.56	0.96	2.66
	O(hcp)	−2.67			
Rh	N(hcp)	−0.48	−3.52	0.38	2.46
	O(fcc)	−2.09			
Pd	N(fcc)	0.24	−2.22	0.20	2.39
	O(fcc)	−1.51			
Ag	N(fcc)	2.97	1.69	0.20	0.83
	O(fcc)	−0.33			
Ir	N(hcp)	−0.21	−2.90	0.28	2.26
	O(fcc)	−1.74			
Pt	N(fcc)	0.43	−1.58	−0.01	1.85
	O(fcc)	−1.06			
Au	N(fcc)	2.59	1.82	−0.14	0.88
	O(fcc)	0.18			

into the rebonding energy and the energy of the intramolecular N–O interaction. For the product state, $E_{\text{int,prod}}$ measures the strength of the repulsive interaction between the co-adsorbed atoms. In the transition state $E_{\text{int,TS}}$ represents the sum of the lateral interactions plus the increased potential energy of the atoms displaced from their equilibrium adsorption sites. Values for the rebonding energy and the interaction energies are compiled in table 2. The rebonding and interaction energies are calculated for N and O atoms in their respective favoured adsorption sites.

The interaction energies calculated for the product states are quite modest, varying for most metallic surfaces between 0.2 and 0.5 eV—hence E_{rebond} calculated from the atomic adsorption energies is already a good approximation to the final-state energies. In the transition state, the intramolecular interaction is quite strong, but the important point is that within the entire group of transition metals, $E_{\text{int,TS}}$ shows only a modest variation between 1.85 eV (Pt) and 2.66 eV (Ru)—as we shall explain in more detail below, this is the basis for the linear PEB relationship. On the heavy noble metals, the intramolecular interaction energy is much weaker, with Cu occupying a place intermediate between the transition metals and the heavy noble metals.

4.2. Transition-state geometries

The modest differences in the intramolecular interaction energies calculated for the transition state reflect the similarity of the transition-state geometries (which are all close to the final-state configurations). Information on the transition-state geometries is given in table 3. The most remarkable aspects are the strong elongation of the N–O bond length compared to the

Table 3. Transition-state geometries for NO dissociation: molecular bond length d_{N-O}, distance h_{S-N} of the N atom above the surface (average z-coordinates of the surface atoms), angle θ between the N–O bond axis and the surface normal, and ν_{N-O} the imaginary value of the molecular stretching frequency in the transition state.

Metal	d_{N-O} (Å)	h_{S-N} (Å)	θ (deg)	ν_{N-O} (cm^{-1})
Co	(1.63)			
Ni	1.69	1.17	78	478
Cu	1.87	1.14	85	423
Ru	1.66	1.30	83	516
Rh	1.77	1.20	80	501
Pd	1.80	1.15	77	511
Ag	2.13	1.20	88	365
Ir	1.94	1.42	77	386
Pt	1.88	1.34	83	428
Au	2.02	1.11	79	394

chemisorbed state and the orientation of the molecule almost parallel to the surface. For all metals, the molecular bond length at the transition state is larger than the distance between two bridge-sites across a hollow (measuring between 1.24 Å on Co(0001) and 1.40 Å on Pt(111) and Au(111)), hence the atoms are already shifted from the bridge sites towards their final positions in the hollows. The distances of both the N and the O atom from the surface are much lower than in the molecular chemisorbed state. Altogether, adsorbate–substrate binding in the transition state shows much more similarity with the binding of the chemisorbed atoms than with the binding of the chemisorbed molecule. There is almost no detailed information on transition-state geometries in the literature. For NO on Pd(111) and Rh(111), our geometries are almost identical to those reported by Loffreda *et al* [7], while Bogicevic and Hass [38] report only a rather modest stretching of the NO bond lengths (by 15% and 30%, respectively) in the TS on Cu(111) and Pt(111), in contrast to our results.

4.3. Comparison with experiments and previous calculations

NO dissociation on several transition-metal surfaces has been studied previously using DFT methods. The most thoroughly studied systems are NO/Pd(111) and NO/Pt(111). For both metals we note good agreement with the calculations of Loffreda *et al* [7] for Pd and of Backus *et al* [21] for Pt, which are based on the same *ab initio* code (VASP) and the same exchange–correlation functional. Minor differences are related to a different surface coverage (higher coverage leading to a slightly enhanced barrier) and a slightly different computational set-up. We also find good agreement with the calculations of Liu *et al* [14], who used a different plane-wave DFT code. Bogicevic and Hass [38] also used VASP for their calculations on NO dissociation on Pt(111), but reported a significantly lower dissociation barrier. Closer inspection of their transition-state geometries shows only a modest stretching on the N–O bond length (0.30 Å or 25%), compared to a much stronger extension of the bond length (by 0.70 Å) in our study. This suggests that their transition-state assignment is based on an interpolation between too coarsely spaced intermediates along the reaction path—the PES profile shown in figure 3 is strongly peaked around the TS. For NO/Pd(111) Hammer [10] reports results obtained using two different functionals, the PW91 [32] and the RPBE [39, 40] gradient-corrected functionals. As already discussed in I, the RPBE functional leads to molecular and dissociative adsorption energies lower by about 0.5 eV than the PW91 functional, but

to almost identical dissociation barriers. For NO/Rh(111) we find excellent agreement of the calculated dissociation barrier with the results of Loffreda *et al* [7] and Hammer and Nørskov [11], although their molecular adsorption energies are slightly lower due to a higher surface coverage. For NO/Ir(111) we even note perfect agreement of our VASP results with the CASTEP calculations of Liu *et al* [14] (for references to the different DFT codes, we refer to I).

Discrepancies with earlier calculations exist for NO dissociation on Cu(111) and on Ru(0001). For NO/Cu(111) Bogicevic and Hass [38] report, as in their calculations for NO/Pt(111), a rather early transition state with a NO bond length stretched by only 15% relative to the molecular chemisorbed state, in contrast to our result of a very late TS. The reasons for the discrepancy with Hammer's [9, 19] results for NO/Ru(0001) remain unclear, but as we shall discuss below our substantially lower dissociation barrier fits much better the general trends across the transition-metal series.

The measurement of the activation energy for dissociation is a complicated problem for both the experiment and theory. Only a very few experimental estimates are available. For NO/Pt(111) Masel [41] reports a dissociation barrier of 1.95 eV from the onset of O_2 desorption in temperature-programmed desorption (TPD) experiments, in reasonable agreement with the DFT results. However, this assignment has been criticized by Bogicevic and Hass [38], who suggested that this value represents the barrier for the recombination of atomic oxygen rather than that for NO dissociation. Pirug and Bonzel [42] measured an activation energy of 1.2 eV for NO dissociation on polycrystalline Pt. Lee *et al* [43] reported an apparent activation energy for NO dissociation on Pt(111) of 0.1 eV, again in reasonable agreement with our calculated transition-state energy.

For NO/Rh(111) Borg *et al* [44] reported an activation energy for dissociation of $E_{\mathrm{diss}} = 0.41$ eV and a desorption energy of 1.22 eV from TPD measurements. The desorption energy corresponds to about 50% of the calculated values; the experimental estimate for the dissociation barrier is in even worse disagreement with theory. However, Root *et al* [45] found a much larger value for the dissociation barrier ($E_{\mathrm{diss}} = 0.83$ eV)—this would again correspond to 50% of the DFT value. Makeev *et al* [46] argued that the consideration of lateral interactions between the adsorbate species in the study by Borg *et al* [44] increases the activation energy from 0.41 to 0.73 eV. For a stepped Rh(111) surface Kruse *et al* [47] reported an activation energy for NO dissociation of 1.06 eV—as the activation energy is generally much lower at steps than on the flat terraces, this would support the DFT result. Thiel *et al* [48] estimated an activation energy of 0.70 eV for dissociation of NO on Ru(0001), in very good (but perhaps coincidental) agreement with our calculated value. Altogether, the scarcity and uncertainty of the experimental estimates hardly allows an assessment of the accuracy of the DFT predictions.

5. Linear free energy relations

Figure 4 shows the variation of the transition-state energies (or apparent activation energies) E_{TS} as a function of the final-state energies (or dissociative chemisorption energies) $E_{\mathrm{ads,N+O}}$. For the group of seven late transition metals we find that a linear Brønsted–Evans–Polanyi (BEP) relation

$$E_{\mathrm{TS}} = A + B \cdot E_{\mathrm{ads,N+O}} \tag{5}$$

with $A = 2.19$ eV and $B = 1.09$ holds with very good accuracy. If the noble metals are included in the linear fit, we find a lower value for the coefficient B, and systematic deviations from the linear BEP relation within the transition-metal series. This is not unexpected, since the interaction of both the molecules and of the dissociated atoms with the substrate is quite

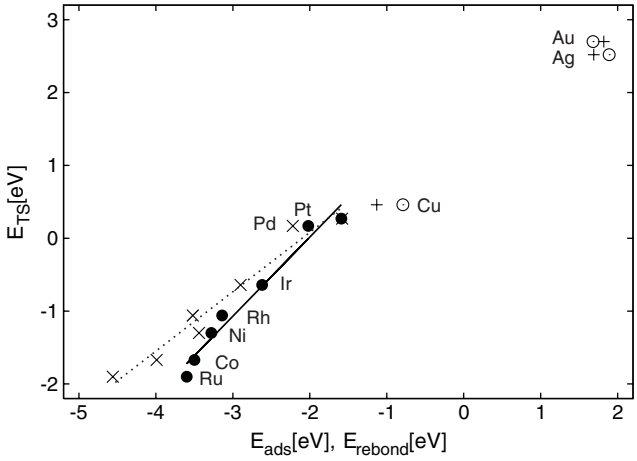

Figure 4. The linear BEP relation between the transition-state energies E_{TS} and the dissociative chemisorption (final-state) energies $E_{\mathrm{ads,N+O}}$ (circles and full line), and between E_{TS} and the sum of the adsorption energies of the isolated atoms, E_{rebond} (crosses and dashed line); cf text.

different for both classes of substrates. It is remarkable that the same BEP relation holds for 3d, 4d, and 5d metals—in contrast to the results of Liu and Hu [16] for CO dissociation on the late 4d and 5d metals, who found a BEP slope close to unity for the 4d metals ($B = 0.98$), but a significantly larger one for the 5d metals ($B = 1.35$).

The quantity linking the dissociative chemisorption energy and the transition-state energy is the activation energy for the reverse reaction, E_{ass}, as

$$E_{\mathrm{TS}} = E_{\mathrm{ass}} + E_{\mathrm{ads,N+O}}. \tag{6}$$

The origin of the linear BEP relations is in the much smaller variation of the activation energies for molecular association (varying only between $E_{\mathrm{ass}} = 1.70$ eV on Ru and $E_{\mathrm{ass}} = 2.19$ on Pd) than of the true activation energy for dissociation (varying between $E_{\mathrm{diss}} = 0.73$ eV on Co and $E_{\mathrm{diss}} = 2.77$ eV) on the various TM surfaces. If the association energies were the same on all substrates, the relationship between the final-state and transition-state energies would be exactly linear. A similar observation holds also for the noble metals. The much weaker substrate dependence of the association energies is a consequence of the similarity of the transition states, as demonstrated by the transition-state geometries described in table 3. Equation (6) also explains why all transition-state energies fit a BEP line with a slope close to 1 ($B = 1.09$), and why the constant A in the BEP relation is close to the average of the activation energies for association.

The activation energy for association is determined by the increase of the intramolecular interaction energy on going from the product to the transition state, $E_{\mathrm{ass}} = E_{\mathrm{int,TS}} - E_{\mathrm{int,prod}}$, with the interaction energies calculated relative to the sum of the atomic adsorption energies calculated relative to the gas-phase NO molecule; see equation (2). This decomposition of the transition-state energies, together with the weak substrate dependence of $E_{\mathrm{int,TS}}$, also suggests a linear dependence of the transition-state energies on the sum of the adsorption energies of the isolated atoms, represented by E_{rebond}, i.e.

$$E_{\mathrm{TS}} = A' + B' \cdot E_{\mathrm{rebond}}. \tag{7}$$

The linear fit shown in figure 4 yields $A' = 1.71$ eV and $B' = 0.81$, hence even atomic adsorption energies can be used for a quite reliable prediction of the activation energies for NO dissociation.

6. Conclusions

Together with the results of molecular NO adsorption on transition and noble metal surfaces presented in I, the present investigation of NO dissociation forms a large database describing the interaction of nitric oxide with close-packed metallic surfaces. Our aim was to achieve a better understanding of the trends governed by the electronic properties of the substrate. In I we have demonstrated that state-of-the-art DFT calculations lead to a consistent picture of geometry and vibrational properties of the molecular adsorbates, while adsorption energies depend on the choice of the exchange–correlation functional and tend to be overestimated in comparison with experiment. Transition-state energies show a much weaker dependence on the choice of the exchange–correlation functional.

NO dissociation is found to be exothermic on Co, Ni, Ru, Rh, and Ir, with a heat of reaction varying between -1.11 eV/molecule on Co and -0.52 eV/molecule on Ir. This is in agreement with the experimental results collected by Broden [1] demonstrating that 3d metals dissociate NO more easily than 4d and 5d metals. On all these surfaces, the transition-state energies (or apparent activation energies) are negative. However, as these metals adsorb molecular NO rather strongly, no direct dissociation can occur; the dissociation process is precursor mediated, with a true activation energy relative to the molecular precursor varying between 0.73 eV on Co and 1.46 eV on Ir. The activation energies are large enough for the coexistence of molecular and dissociated species on Ni, Rh, and Pd.

NO dissociation has a modest endothermic heat of reaction on Pd, Pt, and Cu, so that molecular chemisorption is preferred. Transition-state energies are only weakly positive, so that on heating desorption as well as dissociation will be observed. On these surfaces, adsorbed atomic nitrogen is unstable relative to gas-phase N_2 and will readily undergo recombinative desorption, while atomic oxygen is still bound to the surface. Finally, on Ag and Au surfaces, NO dissociation is strongly endothermic.

We have demonstrated a linear Brønsted–Evans–Polanyi relationship between the final-state energies and the transition-state energies for NO dissociation. The origin of the linear BEP relation is in the small substrate dependence of the activation energy for the reverse process, the associative formation of NO molecules from adsorbed atomic N and O. The weak substrate dependence of the association energies in turn originates from the similarity of the transition and final states: we have demonstrated that relative to the molecular precursor states the N–O bond lengths in the transition states are stretched by 0.43 Å (Co) and 0.74 Å (Ir) and that the orientation of the molecule is almost parallel to the surface. Our results extend the evidence for the validity of a BEP relationship for the dissociation of diatomic molecules. Our investigations have been restricted to close-packed surfaces—the influence of the surface geometry on the dissociation reactions was outside the scope of our investigations. Results for NO dissociation on stepped and kinked surfaces have been reported for Pd, Ru and Pt surfaces (see introduction for details). At steps and kinks the bonding competition between the atoms is reduced, leading to a stronger bonding in the transition as well as in the final states. As a result, the slope of the BEP line remains essentially the same, but the line is shifted to lower energies.

References

[1] Brodén G, Rhodin T, Bruckner C, Benbow R and Hurych Z 1976 *Surf. Sci.* **59** 593
[2] Brown W A and King D A 2000 *J. Phys. Chem.* B **104** 2578
[3] Parvulsecu V I, Grange P and Delmon B 1998 *Catal. Today* **46** 233
[4] Burch R, Breen J P and Meunier F C 2002 *Appl. Catal.* **39** 283

[5] Gajdos M, Eichler A and Hafner J 2004 *J. Phys.: Condens. Matter* **16** 1141
[6] Gajdos M, Eichler A and Hafner J 2006 *J. Phys.: Condens. Matter* **18** 13
[7] Loffreda D, Simon D and Sautet P 2003 *J. Catal.* **213** 211
[8] Hammer B 1998 *Faraday Discuss.* **110** 323
[9] Hammer B 1999 *Phys. Rev. Lett.* **83** 3681
[10] Hammer B 2001 *J. Catal.* **199** 171
[11] Hammer B and Nørskov J K 2000 *Adv. Catal.* **45** 71
[12] Eichler A and Hafner J 2001 *Chem. Phys. Lett.* **343** 383
[13] Eichler A and Hafner J 2001 *J. Catal.* **204** 118
[14] Liu Z P, Jenkins S J and King D A 2003 *J. Am. Chem. Soc.* **125** 14660
[15] Liu Z P, Jenkins S J and King D A 2004 *J. Am. Chem. Soc.* **126** 10746
[16] Liu Z P and Hu P 2001 *J. Chem. Phys.* **114** 8244
[17] Dahl S, Logadottir A, Jacobsen C J H and Nørskov J K 2001 *Appl. Catal.* A **222** 19
[18] Logadottir A, Rod T H, Nørskov J K, Hammer B, Dahl S and Jacobsen C J H 2001 *J. Catal.* **197** 229
[19] Hammer B 2000 *Surf. Sci.* **459** 323
[20] Ge Q and Neurock M 2004 *J. Am. Chem. Soc.* **126** 1551
[21] Backus E H G, Eichler A, Grecea M L, Kleyn A W and Bonn M 2004 *J. Chem. Phys.* **121** 7946
[22] Michaelides A, Liu Z P, Zhang C J, Alavi A, King D A and Hu P 2003 *J. Am. Chem. Soc.* **125** 3704
[23] Bligaard T, Nørskov J K, Dahl S, Matthiesen J, Christensen C H and Sehested J 2004 *J. Catal.* **224** 206
[24] Bronsted N 1928 *Chem. Rev.* **5** 231
[25] Evans M G and Polanyi N P 1936 *Trans. Faraday Soc.* **34** 11
[26] Hammond G S 1955 *J. Am. Chem. Soc.* **77** 334
[27] http://cms.mpi.univie.ac.at/vasp/
[28] Kresse G and Furthmüller J 1996 *Phys. Rev.* B **54** 11169
[29] Blöchl P 1994 *Phys. Rev.* B **50** 17953
[30] Kresse G and Joubert D 1999 *Phys. Rev.* B **59** 1758
[31] Perdew J P and Zunger A 1981 *Phys. Rev.* B **23** 5048
[32] Perdew J P, Chevary J A, Vosko S H, Jackson K A, Pederson M R, Singh D J and Fiolhais C 1992 *Phys. Rev.* B **46** 6671
[33] Press W, Teukolsky S, Vetterling W and Flannery B 2002 *Numerical Recipies in C++* (New York: Cambridge University Press)
[34] Mills G, Jónsson H and Schenter G K 1995 *Surf. Sci.* **324** 305
[35] Ulitsky A and Elber R 1990 *J. Chem. Phys.* **92** 1510
[36] Henkelmann G, Uberuaga B P and Jonsson H 2000 *J. Chem. Phys.* **113** 9901
[37] Maragakis P, Andreev S A, Brumer Y, Reichman D R and Kaxiras E 2002 *J. Chem. Phys.* **117** 4651
[38] Bogicevic A and Hass K C 2002 *Surf. Sci.* **506** L237
[39] Perdew J P, Burke K and Ernzerhof K 1996 *Phys. Rev. Lett.* **77** 3865
[40] Hammer B, Hansen L B and Nørskov J K 1999 *Phys. Rev.* B **59** 7413
[41] Masel R I 1986 *Cat. Rev. Sci. Eng.* **28** 335
[42] Pirug G, Bonzel H P, Hopster H and Ibach H 1979 *J. Chem. Phys.* **71** 593
[43] Lee S B, Kang D H, Park C Y and Kwak H T 1995 *Bull. Korean Chem. Soc.* **16** 157
[44] Borg H J, Reijerse J-J, van Santen R A and Niemantsverdriet J W 1994 *J. Chem. Phys.* **101** 10052
[45] Root T W, Fisher G B and Schmidt L D 1988 *J. Chem. Phys.* **85** 4679
[46] Makeev A G and Slinko M M 1996 *Surf. Sci.* **359** L467
[47] Kruse N 1990 *J. Vac. Sci. Technol.* A **10** 3432
[48] Thiel P A, Weinberg W H and Yates J T 1979 *Chem. Phys. Lett.* **67** 403